Journal of Electronics, Electromedical Engineering, and Medical Informatics
Homepage: jeeemi.org; Vol. 7, No. 4, October 2025, pp: 1144-1157 e-ISSN: 2656-8632

RESEARCH ARTICLE OPEN ACCESS

A PSO-SVM-Based Approach for Classifying ECG and EEG Bio signals in Seizure Detection

Zougagh Lahcen, Bouyghf Hamid, and Nahid Mohammed

Laboratory of Engineering Sciences and Biosciences, Faculty of Sciences and Techniques, Hassan II University, Mohammedia, Morocco

Corresponding author: Zougagh Lahcen. (e-mail: lahcen.zougagh-etu@etu.univh2c.ma), **Author(s) Email**: Bouyghf Hamid (e-mail: hamid.bouyghf@gmail.com, Nahid Mohammed (e-mail: mohammed.nahid@gmail.com)

Abstract **Early identification of epileptic activities is essential for clinical analysis and preventing advancement of the disease. Despite the development of neurological diagnostic techniques, the current analysis of epileptic seizures is still relying on a visual interpretation of electroencephalogram (EEG) signal. Neurology specialists manually perform this examination to detect patterns, a process that is both challenging and time-consuming. Biomedical signals, such as EEG and electrocardiogram (ECG), are important tools for studying human brain disorders, particularly epilepsy. This paper aims to develop a system that automatically detects epileptic seizures using discrete wavelet decomposition (DWT), particle swarm optimization (PSO), and support vector machine (SVM), thereby relieving clinicians of their challenging tasks. The proposed system employs the DWT method, PSO, and SVM. This approach has three steps. First, we introduce a method that uses a four-level discrete wavelet transform (DWT) to extract important information from electroencephalogram and electrocardiogram signals by breaking them down into useful features. Second, we optimize the SVM classifier parameters using the PSO algorithm. Finally, we classify the extracted parameters using the optimized SVM. The system achieves an average accuracy of 97.92%, a 100% recall, a 96.15% specificity, and a 0.96 AUC value. Our findings demonstrate the success of this method, showing that the PSO-optimized SVM performs significantly better in classification. In addition, our findings also demonstrate the importance of using ECG signals as supplemental data. One implication of our work is the potential for creating wearable, real-time, customized seizure warning systems. In the future, these systems will be deployed on embedded platforms in real time and validated using larger datasets.**

Keywords **ECG, DWT, EEG, Support vector machine, Particle swarm optimization, Classification.**

I. Introduction

Epilepsy is a long-term neurological health disorder most often linked to recurrent, sudden, and spontaneous seizures generated from irregular electrical activity in the human brain [1]. As reported by the World Health Organization, about 50 million people develop epilepsy each year, making it one of the most popular neurological illness worldwide [2]. The random occurrence of seizures negatively impacts the daily lives of those with epilepsy, which means that effective diagnostic and treatment methods are needed [3].

The EEG is the primary diagnostic instrument for epilepsy; the detection of transient electrical irregularities during seizures facilitates such evaluations [4]. Conversely, manual interpretation of EEG data is an arduous task requiring neurologists' expertise, which may not always be accessible in clinical environments [5]. Therefore, automated seizure detection devices are needed for quick diagnosis and action. For the last few decades, a lot of money has been spent on using artificial intelligence to automate seizure detection in the area of epilepsy research [6]. The use of machine learning in seizure identification has grown even faster since doctors started using it to look at patients' EEGs to determine neurological problems [7]. EEG signals are difficult to study due to their nonlinear and nonstationary characteristics [8]. Despite this difficulty, EEG signals are a promising method for detecting epileptic seizures. During seizures, EEG measurements exhibit irregular, synchronized spikes and sudden wave discharges [9].

Prior investigations into seizure identification via electroencephalogram (EEG) signals have explored diverse techniques for modification, transformation, and extraction of critical data [10]. These analyses investigated both machine learning and deep learning methods. For instance, previous study [11] employed empirical mode decomposition (EMD) to examine EEG data. On the other hand, others [12] and [13] used wavelet transformation and Tunable Q-Wavelet Transform (TQWT), respectively, with the data split into frequency sub bands. Other research utilized unprocessed EEG recordings as input data [14], [15],

Manuscript received 12 June 2025; Revised 25 August 2025; Accepted 10 September 2025; Available online 30 September 2025
Digital Object Identifier (**DOI**): https://doi.org/10.35882/jeeemi.v7i3.1159
Copyright © 2025 by the authors. This work is an open-access article and licensed under a Creative Commons Attribution-ShareAlike 4.0 International License (CC BY-SA 4.0).

[16]. Scientists have used convolutional neural networks (CNNs) on raw signals to make new features [17] and graph attention networks (GATs) to acquire spatial features [18]. Moreover, novel investigations are underway to identify superior methods for extracting significant information from original EEG signals [19]. Most of the research on using EEG to determine epileptic seizures has been about breaking down signals and getting important features out of them so that machine and deep learning methods can work better at finding seizures [20]. The study referenced as a previous study [21] utilized a fusion of discrete wavelet transforms and support vector machines (SVM) to extract characteristics from EEG signals and categorize them, achieving significant precision in detecting epileptic seizures.

Electrocardiography (ECG) has become a significant adjunctive modality. Seizures often cause changes in the nervous system that can alter heart rate, heart rate variability, and ECG waveform shape [22]. Many clinical studies have shown that ECG reliably find autonomic dysfunction related to seizures, which may occur prior to EEG abnormalities. Combining EEG and ECG data creates a multimodal framework that utilizes the strengths of both types of data [23]. EEG detects direct cortical abnormalities, while ECG indicates systemic physiological alterations associated with seizures. By combining these signals, detection models can lower false alarms, increase sensitivity, and provide a more complete picture of seizure dynamics. This research builds on this rationale by introducing a combined EEG-ECG methodology and substantiating the additional benefits of ECG through comparative experiments.

To improve SVM classification work, higher accuracy means two different things. First, a straightforward and intuitive method for extracting features is presented. The second part is about using the suggested feature-extraction method in a better PSO-SVM framework. This framework uses particle swarm optimization and support vector machines to increase accuracy, shorten training time, and test how well the feature-extraction method works. This method makes PSO's contribution to the global search process better by making the population more diverse. We make the most of the improved PSO method to adjust the SVM parameters, which makes the model work better and allows us to generalize better.

The outline of this paper is as follows: Section II describes the overall methodologies. Section III covers the dataset, DWT decomposition, the PSO optimization technique, and the SVM classifier. Section IV presents the achieved results and compares them with those of alternative methods. Section V interprets the findings and their implications for clinical practice and discusses the limitations of the research. Finally, Section VI concludes the paper and proposes further research.

II. Method

A. Main methodology

This section provides a full review of the ECG and EEG data sets utilized, as well as an explanation of the analysis methodologies used for these signals. Fig. 1 shows how four main processes are carried out to develop an automated tool for identifying neurological brain problems. The method consists of acquiring EEG and ECG data, pre-processing them, extracting significant information and performing classification and decision-making. A preprocessing module examines, modifies, and splits the EEG and ECG data collected. The Discrete Wavelet Transform (DWT) method decomposes the signal into its constituent; D1,

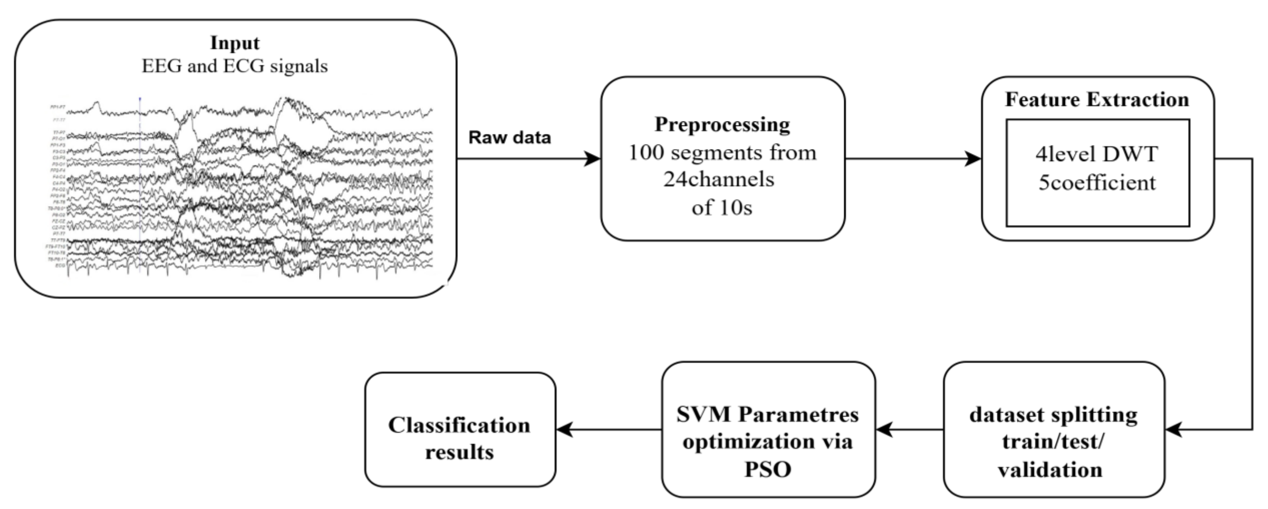

Fig. 1. The suggested approach block diagram

Manuscript received 12 June 2025; Revised 25 August 2025; Accepted 10 September 2025; Available online 30 September 2025
Digital Object Identifier (DOI): https://doi.org/10.35882/jeeemi.v7i3.1159
Copyright © 2025 by the authors. This work is an open-access article and licensed under a Creative Commons Attribution-ShareAlike 4.0 International License (CC BY-SA 4.0).

D2, D3 and D4. We further derived feature vectors by computing several parameters, among them standard deviation, energy, skewness, mean, kurtosis, variance and entropy. We classified the collected features using an SVM algorithm. We executed and validated a number of different combinations of the proposed ideas. We evaluated the proposed approaches using MATLAB software. The remaining sections present an extensive examination and elucidation of each phase, which includes data description and classification methodology.

B. Data Collection

This study used a publicly available CHB-MIT dataset from Children's Hospital Boston, USA [24]. The CHB-MIT dataset provider of data collected from individuals with inextricable seizures [25]. The dataset contains 24 cases collected from a sample of 23 individuals. Denominated 'chb01' through 'chb24', the cases showcase extensive EEG recordings taken over several days from individuals undergoing evaluation as potential surgical candidates. Each case consists of several consecutive electroencephalogram (EEG) signal stored in .edf file format. This study uses recording data from 23 EEG channels and one ECG channel obtained from a subject identified as 'chb04'. To improve the balance of the introduced automated method, we selected EEG and ECG bio signals from the CHB-MIT freely available in https://doi.org/10.13026/C2K01R.,including at the same time epileptic and non-epileptic cases [26].
All signals in the dataset were collected at a frequency of 256 samples per second with a 16-bit resolution. The recordings used the worldwide 10–20 method for EEG electrode placement and terminology.

C. Preprocessing

This research used a 10-second non-overlapping window to split the signal from the channels. The rationale for using a 10-second frame is because segments that are too tiny or vast may result in less accurate categorization. Segments that are too tiny may lack sufficient useful patterns for the captured features, while segments that are very lengthy may obscure the true patterns within the data [27]. Before extracting the features, the EEG and ECG signals were cleaned up to get rid of baseline drifts and noise at high frequencies. We used a 4th-order Butterworth band-pass filter (0.5–40 Hz) on the EEG recordings to keep clinically important rhythms (delta to gamma), while getting rid of low-frequency drifts and muscle artifacts. The ECG recordings were done with a band-pass filter that let through the frequencies from 0.5 to 45 Hz. This kept the shape of the signal while getting rid of baseline wander and power-line noise.

D. Feature extraction

The study selected the discrete wavelet transform (DWT) for feature extraction because of the inherent limitations of time-frequency analysis techniques. The Fourier transform (FT) is limited by signal stationarity, a condition that is rarely met by transient-rich, non-stationary signals like the EEG and ECG. The Short-Time Fourier Transform (STFT) addresses this issue, but it introduces a fixed resolution trade-off. Empirical mode decomposition (EMD) is adaptive, yet it has been criticized for its computational intensity, susceptibility to noise, and mode mixing [28]. DWT offers superior time localization for high-frequency transients and frequency localization for slower oscillations, making it a compelling choice for feature extraction.

1. Fourier Transform (FT)

The Fourier Transform provides a global frequency-domain representation of a signal, assuming stationarity over the entire duration. It is defined as in Eq. (1) [29]:

$$X(f) = \int_{-\infty}^{+\infty} x(t)e^{-j2\pi ft}dt \tag{1}$$

where $x(t)$is the time-domain signal and $X(f)$is its spectral representation [29]. Although it is powerful, the FT does not provide information about the temporal localization of frequency components, which limits its applicability for non-stationary signals such as EEG and ECG.

2. Short-Time Fourier Transform (STFT)

To address the lack of time localization in FT, the Short-Time Fourier Transform applies a sliding window $w(t)$ to the signal, allowing frequency analysis within localized time segments. The STFT is expressed in Eq. (2) [29]as:

$$X(t,f) = \int_{-\infty}^{+\infty} x(\tau)w(\tau - t)e^{-j2\pi f\tau}d\tau \tag{2}$$

where $w(t)$ is a window function that defines the local time segment. The STFT provides a time–frequency representation, but its resolution is limited by the fixed window size: narrow windows give good time resolution but poor frequency resolution, while wide windows have the opposite effect [29].

3. Discrete wavelet transform

For spectral analysis of non-stationary data, the wavelet transform is better than other methods. The wavelet can change the size of the window by making it bigger for low frequencies and smaller for high frequencies. This lets you capture the entire frequency spectrum with the best time-frequency resolution. Discrete wavelet transforms assess signals across multiple scales [30]. Fig. 2 shows how the discrete wavelet transform looks at the signal at different levels

Manuscript received 12 June 2025; Revised 25 August 2025; Accepted 10 September 2025; Available online 30 September 2025
Digital Object Identifier (**DOI**): https://doi.org/10.35882/jeeemi.v7i3.1159
Copyright © 2025 by the authors. This work is an open-access article and licensed under a Creative Commons Attribution-ShareAlike 4.0 International License (CC BY-SA 4.0).

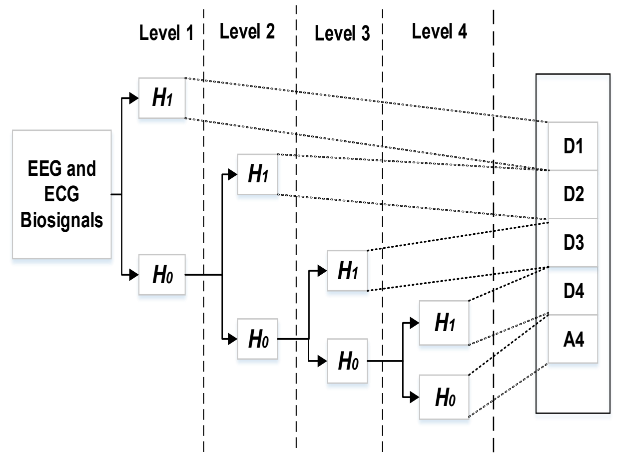

Fig. 2. Discrete wavelet transform method

of detail. Choosing the right number of detection levels and the right decomposition level is important for getting accurate signal analysis. The decomposition level affects how well categorization works by deciding which wavelet type and main frequency components to use. The process entails the collection of EEG and ECG data, preprocessing, feature extraction, classification, and decision-making. Wavelet decomposition operates by applying a pair of complementary filters to iteratively decompose the original time series into distinct frequency sub-bands. The process is first governed by the scaling and shifting parameters *a* and *b*. The general formulation of the wavelet transform is expressed in Eq. (3) [31]: constrained by

$$W(a,b)=\frac{1}{\sqrt{|a|}}\int_{-\infty}^{+\infty}x(t)\psi\left(\frac{t-b}{a}\right)dt,\quad a,b\in S,\quad a>0 \tag{3}$$

where $x(t)$ is the input signal, $\psi(t)$ is the mother wavelet, and *a* and *b* are the scale and translation parameters, respectively. At each stage of decomposition, the low-pass filter H_0 extracts the approximation coefficients, corresponding to low-frequency components that capture activity over broader time scales, while the high-pass filter H_1 produces the detail coefficients, isolating high-frequency variations that highlight transient dynamics [31]. This principle is formalized in Eq. (4) [31], where the discrete wavelet functions are defined as

$$\psi_{j,k}(t)=\frac{1}{\sqrt{2^j}}\psi\left(\frac{t-k2^j}{2^j}\right) \tag{4}$$

and the hierarchical signal representation is expressed as Eq. (5) [31]

$$x(t)=\sum_k A_j(k)\phi_{j,k}+\sum_j\sum_k D_j(k)\phi_{j,k} \tag{5}$$

Through successive iterations of $H_0$and H_1, this filter bank framework yields a multiresolution analysis that progressively captures both long-term rhythmic activity and short-lived oscillations. Such a decomposition is particularly effective for EEG and ECG signals, where clinically relevant information resides simultaneously in low-frequency background rhythms and high-frequency transient features.

The Daubechies wavelet family (db4) is used to break down EEG and ECG signals into their parts using the DWT. The db4 wavelet is frequently cited in literature as highly effective for the analysis of non-stationary biomedical signals, particularly in capturing transient oscillations such as epileptic discharges. It is helpful for finding sudden changes in signals while reducing boundary artifacts because it has a small support, is orthogonal, and looks like EEG waveforms. Early tests showed that db4 created stable and unique features, which made it possible for the proposed system to reliably classify the data.

A preprocessing module utilized a four-level DWT to analyze and decompose the collected EEG and ECG signals. This decomposition, which resulted in detail coefficients D1, D2, D3, and D4, was chosen based on prior studies indicating that four levels attain an optimal balance between capturing physiologically relevant frequency information and reducing signal fragmentation. This level of decomposition separates the delta (0.5–4 Hz), theta (4–8 Hz), alpha (8–13 Hz), beta (13–30 Hz), and low-gamma (30–40 Hz) frequency bands. These are the bands where seizures happen.

To improve the analysis of the impact of seizures on cardiac and cerebral function, we suggested augmenting seizure classification with the discrete wavelet transform, facilitating the differentiation between seizure and non-seizure states. We chose two parts of each activity for test evaluation: one from the normal phase and one from the epileptic event. Fig. 3 and Fig. 4 show the full results of using the four-level discrete wavelet transform on two ECG and two EEG segments. The first segment comes from activity that is not epileptic, while the second segment is called the epileptic phase. An examination of these data reveals an elevation in signal amplitude and frequency during the seizure, in contrast to the non-epileptic signal segments.

4. Extracted features

Feature extraction is crucial in signal processing, especially for interpreting EEG and ECG data. These features make up the basic parts of a signal and let us get useful information from data that has not been processed yet [32]. The features of EEG signals can give us important information about the brain's health, such as finding unusual activity patterns that are linked

Manuscript received 12 June 2025; Revised 25 August 2025; Accepted 10 September 2025; Available online 30 September 2025
Digital Object Identifier (**DOI**): https://doi.org/10.35882/jeeemi.v7i3.1159
Copyright © 2025 by the authors. This work is an open-access article and licensed under a Creative Commons Attribution-ShareAlike 4.0 International License (CC BY-SA 4.0).

to epilepsy or other neurological diseases. We then used these features to look into things more and to give machine learning algorithms information they need to do things like categorize, predict, or do other kinds of analysis. The robustness of extracted features. As a result, feature extraction is a very important part of the whole process [33]. To calculate the absolute mean of each row in the generated EEG and ECG data, we aggregate all the absolute values of the elements and then divide by the total number of elements in each row. The absolute mean is calculated by Eq. (6) [34]

$$m_x = \frac{1}{A}\sum_{a=1}^{A}|X_a| \tag{6}$$

m_x represents the absolute means of values, A corresponds to the number of samples, and $|X_a|$ represents the absolute value of EEG/ ECG sample in nth sample. Variance is calculated by Eq. (7) [34]

$$s_x^2 = \frac{1}{A-1}\sum_{a=1}^{A}(X_a - m_x) \tag{7}$$

A represents the number of samples, $X_a$represents the EEG/ECG in αth sample,s_x^2 represents the variance, and m_x represents the means of values. Skewness is calculated by Eq. (8) [34]

$$sk = \frac{1}{(A-1)\sigma_x^3}\sum_{a=1}^{A}(X_a - m_x)^3 \tag{8}$$

A represents the number of samples, $X_a$represents the EEG/ECG in αth sample, m_x represents the means of values, and σ_x represents the Standard deviation. Kurtosis is calculated by Eq. (9) [34].

$$kr = \frac{1}{(A-1)\sigma_x^4}\left(\sum_{a=1}^{A}(X_a - m_x)^4\right) - 3 \tag{9}$$

A represents the number of samples, $X_a$represents the EEG/ECG in αth sample, m_x represents the means of values, and σ_x represents the standard deviation. In Eq. (10) [30] and Eq. (11) [30], the quantified energy is deliniated for an EEG and ECG segments, respectively, as follows:

$$E_{\text{EEG10}}\,(i,n) = \textstyle\sum_{K=1}^{L}|EEG(i,K)|^2 \tag{10}$$

$$E_{\text{ECG10}}\,(n) = \textstyle\sum_{K=1}^{L}|ECG(K)|^2 \tag{11}$$

L represent the record's and *i* denotes the channel number. In Eq. (12) [33] and Eq. (13) [33], the standard deviations of the EEG and ECG signals are defined, respectively, as follows:

$$\sigma_{EEG10}(i,n) = \left(\tfrac{1}{L}\textstyle\sum_{K=1}^{L}(EEG(i,K) - \overline{EEG(i)})^2\right)^{\frac{1}{2}} \tag{12}$$

$$\sigma_{ECG10}(n) = \left(\tfrac{1}{L}\textstyle\sum_{K=1}^{L}(ECG(K) - \overline{ECG(n)})^2\right)^{\frac{1}{2}} \tag{13}$$

III. PSO-SVM approach

A. SVM CLASSIFIER

SVM demonstrates exceptional generalization capabilities by autonomously identifying support vectors to form a hyperplane for classification, guided by VC dimension analysis and the basic principle of reducing structural risk. In addition, SVM solves the problems of network architecture selection, overfitting, under fitting, and other challenges associated with artificial neural networks and similar methods. The primary approach of the SVM algorithm is to perform a nonlinear transformation of the entering data from a low-

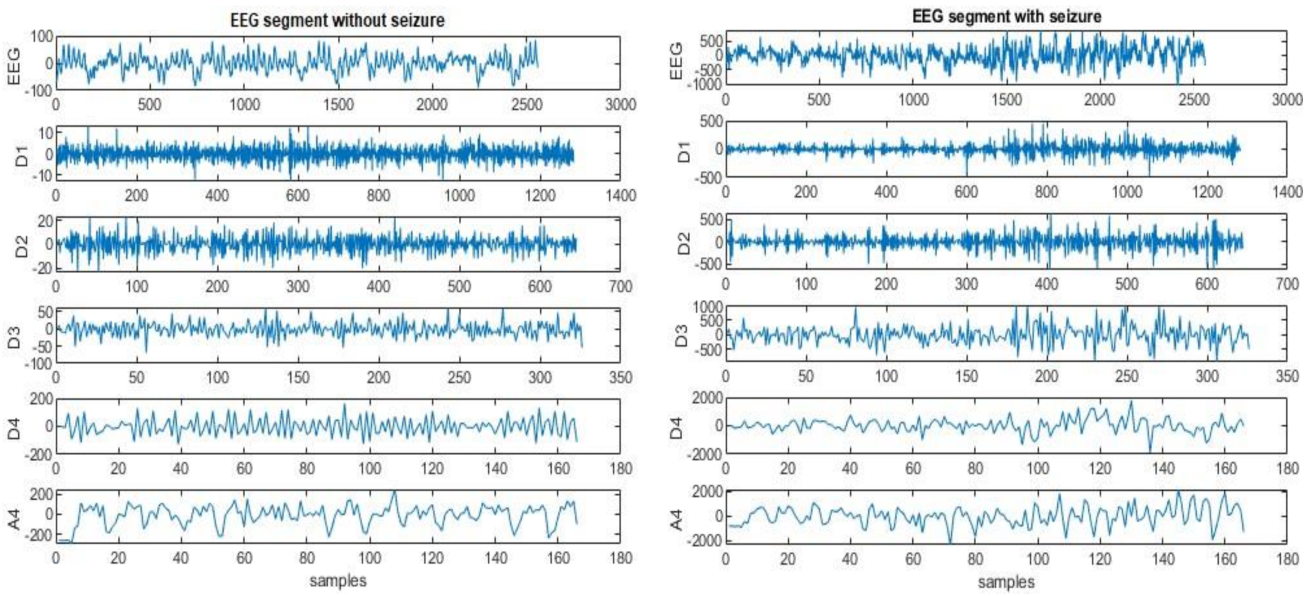

(a) (b)

Fig. 3. Application of DWT on EEG segments (a) Segment without seizure **(b)** Segment with seizure

Manuscript received 12 June 2025; Revised 25 August 2025; Accepted 10 September 2025; Available online 30 September 2025
Digital Object Identifier (**DOI**): https://doi.org/10.35882/jeeemi.v7i3.1159
Copyright © 2025 by the authors. This work is an open-access article and licensed under a Creative Commons Attribution-ShareAlike 4.0 International License (CC BY-SA 4.0).

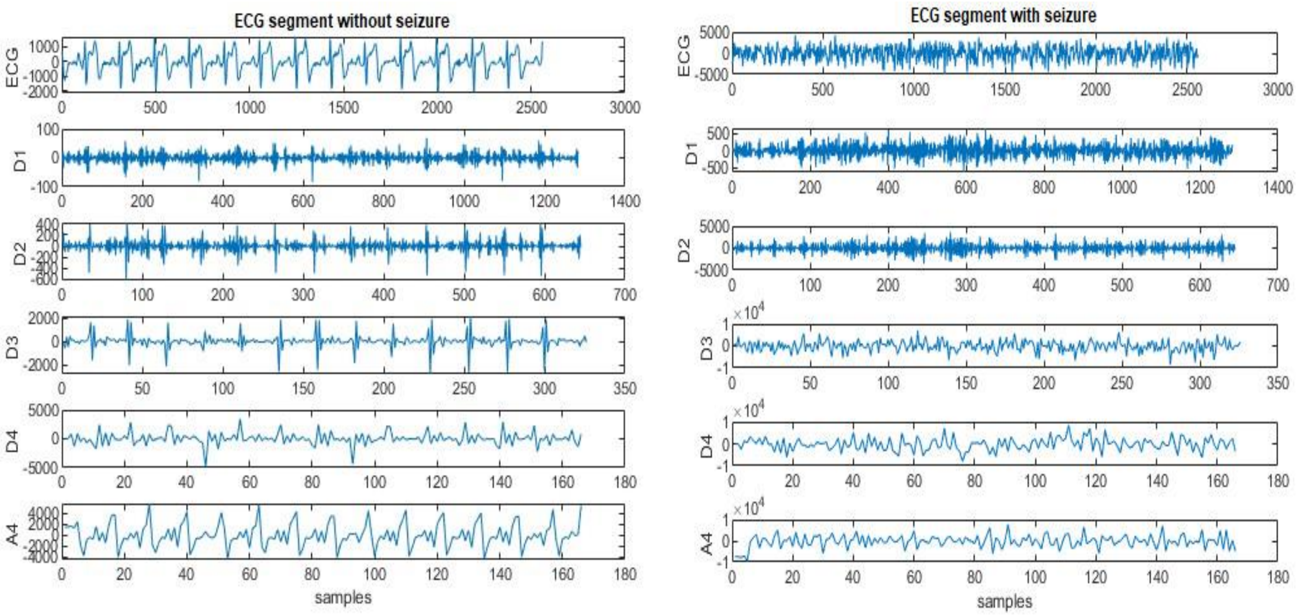

(a) (b)

Fig. 4. Application of DWT on ECG segments (a) Segment without seizure (b) Segment with seizure

dimensional domain to a high-dimensional feature domain, where it achieves linear separating ability [35].

SVM uses the most efficient classification hyperplane *f(x)* presented by Eq. (14) [35] to classify samples and refers to the two samples closest to this hyperplane as support vectors. The sum of the distances across the support vectors from the optimal hyperplane is 2*w*. The structural risk minimization principle dictates maximizing this sum. Consequently, the task of finding the optimal hyperplane reduces to solve the subsequent optimization issue.

$$f(x) = w^T x + b = 0 \tag{14}$$

The function f(x) denotes the separating hyperplane, whereas the parameter w corresponds to the weight and b represents the bias. In the presence of a linearly indistinguishable issue, the equation mentioned above must be expanded by including the slack variable ξi and the penalty c component. This modification enables the creation of a model capable of resolving the nonlinear problem. The resulting equation is Eq. (15) [35] presented as follows:

$$\begin{cases} min \frac{1}{2}\|w\|^2 + c\sum_{i=1}^{n}\xi_i \\ s.t.\, y_i(wx_i + b) + \xi_i - 1 \geq 0, \quad \xi_i \geq 0; i = 1,2,\cdots,n \end{cases} \tag{15}$$

The equation is then converted to a dual problem via the Lagrange multiplier method, thereby obtaining the decision function Eq. (16) [35] as follows:

$$f(x) = sign\left(\sum_{i,j=1}^{n} a_i y_i k(x_i, x_j) + b\right) \tag{16}$$

This study utilized the radial basis as the selected kernel function and used the PSO technique and the modified PSO algorithm to ascertain the best penalty value C and kernel parameter γ. The radial basis kernel function Eq. (17) [35] is articulated as follows:

$$k(x_i, x_j) = e^{\left(-\gamma\|x_i - x_j\|^2\right)} \tag{17}$$

where c is the parameter of RBF that specifies the size of the kernel. In most cases, c varies from 0 to 1.

In this context, γ represents the size of the kernel function. From the derivation process, it is clear that the values of penalty factor c and kernel function size γ are key factors influencing the identification performance of SVM. In the current classification, increasing c may decrease the generalizing ability of the SVM classifier, while decreasing c may result in under fitting. The parameter γ is a reflection of the distribution of the original data when it is projected into a high-dimensional domain. If γ is too wide, the projection of the kernel function in the high-dimensional domain will shrink, which will reduce the effectiveness of the classifier in dealing with non-linearly separable data [36]. On the other hand, if γ is too small, the projection area in the high-dimensional domain is slightly expanded, which weakens the generalization ability of the classifier. Therefore, the determination of the optimal values of the penalty factor c and the width of the kernel function γ is crucial for the improvement of the recognition accuracy.

The Radial Basis Function (RBF) kernel was selected for the Support Vector Machine (SVM) classifier because it is theoretically sound and has been shown to work well with the complex feature spaces of

Manuscript received 12 June 2025; Revised 25 August 2025; Accepted 10 September 2025; Available online 30 September 2025
Digital Object Identifier (**DOI**): https://doi.org/10.35882/jeeemi.v7i3.1159
Copyright © 2025 by the authors. This work is an open-access article and licensed under a Creative Commons Attribution-ShareAlike 4.0 International License (CC BY-SA 4.0).

EEG and ECG signals during seizures. Preliminary comparative analyses confirmed this selection, showing that a linear kernel was insufficient due to its unrealistic presumption of linear separability and that a polynomial kernel was susceptible to variations in degree and regularization parameters. These factors resulted in suboptimal generalization and higher computing costs.

B. PSO algorithm

The PSO method, initially developed by Kennedy and Eberhart in 1995 and subsequently refined by Chen et al. in 2017, is a population-based locating algorithm that employs a model of natural behavior observed in birds in a flock. The PSO method entails navigating particles (individuals) across a hyper dimensional search space [37], [38]. Individuals' social-psychological tendency to undermine others' achievements influences the placement of particles within the search area. The particle's accumulated experience and knowledge influence its behavior within the swarm. Modeling this social behavior has the consequence of conducting the search in a manner that revisits previously successful locations within the search space. Specifically, the following equations will modify each particle's location (x) Eq. (18) [37] and velocity (v) Eq. (19) [37].

$$x_{ij}(t) = x_{ij}(t-1) \leftrightarrow +v_{ij}(t) \tag{18}$$

$$v_{ij}(t) = wv_{ij}(t-1) + c_1 r_1 \left(P_{best_{ij}} - x_{ij}(t)\right) + c_2 r_2 \left(G_{best_{ij}} - x_{ij}(t)\right) \tag{19}$$

The symbol $V_{ij}(t)$ represents particle *i*'s velocity at iteration *j*, while $X_{ij}(t)$ represents the particle *i*'s location at iteration *j*. The inertia weight is employed to manage the impact of the velocity's past behavior. The symbol *t* represents the iteration number, *t*. The cognitive learning component, C_1, indicates the cognitive learning component, while the social learning factor, C_2, represents the social learning factor. Finally, the random values r_1 and r_2, which indicate remembering capacity, are represented by the symbols r_1 and r_2, respectively. PSO terminates either when the maximum number of generations is achieved or when a particle's optimal position within the swarm cannot be improved after a significant number of generations. The important parameters of PSO used in this model are given in Table 1.

Table 1. PSO characteristics

Parameter	Value
particles	50
C1	1.5
C2	1.5
W1	0.4
W2	0.9
iteration	100

C. PSO-SVM combined approach

As illustrated in Fig. 5, the suggested method employs the combination of PSO-SVM for classifying datasets subsequent to feature extraction. The chosen kernel for the SVM classifier is the RBF kernel. We used an innovative particle swarm optimization method to ascertain the appropriate penalty factor C and parameter g inside the SVM kernel function. The process of implementing the combined PSO-SVM is presented in Algorithm 1.

Algorithm 1. PSO-SVM Optimization for Epileptic Seizure Detection

(1) **Input:** Training dataset, swarm size *N*, max iteration T
(2) **Output:** optimized SVM parameters (C^*, γ^*)
(3) Initializion
(4) For each particle $i \in \{1,2,\dots,N\}$, $x_i(0) = (C_i, \gamma_i)$
(5) Set initial velocities v_j for each particle p_j
(6) Evaluate fitness using SVM classification accuracy Eq. (20)
(7) Assign each particle's personal best $pbest_j$
(8) Identify the global best particle $gbest$
(9) $t \leftarrow 0$
(10) **DO**
(11) **FOR** each particle p_j
(12) Update Position using Eq. (18)
(13) Update velocity using Eq. (19)
(14) Train SVM with parameters $(C, \gamma) = p_j(t+1)$
(15) Evaluate fitness of $p_j(t+1)$
(16) Update $pbest_j$
(17) **END FOR**
(18) Update global best $gbest$
(19) **While** $t = T$
(20) Return best solution $g = (C^*, \gamma^*)$
(21) Retrain SVM with (C^*, γ^*)
(22) Perform final classification result

The implementation of a careful strategy for data partitioning and validation was essential for ensuring full testing of the model's robustness and generalizability. The dataset was split into three parts: 70% for training, 15% for validation, and 15% for holdout evaluation. A strict protocol for separating patients was employed to ensure that no patient's data

Manuscript received 12 June 2025; Revised 25 August 2025; Accepted 10 September 2025; Available online 30 September 2025
Digital Object Identifier (**DOI**): https://doi.org/10.35882/jeeemi.v7i3.1159
Copyright © 2025 by the authors. This work is an open-access article and licensed under a Creative Commons Attribution-ShareAlike 4.0 International License (CC BY-SA 4.0).

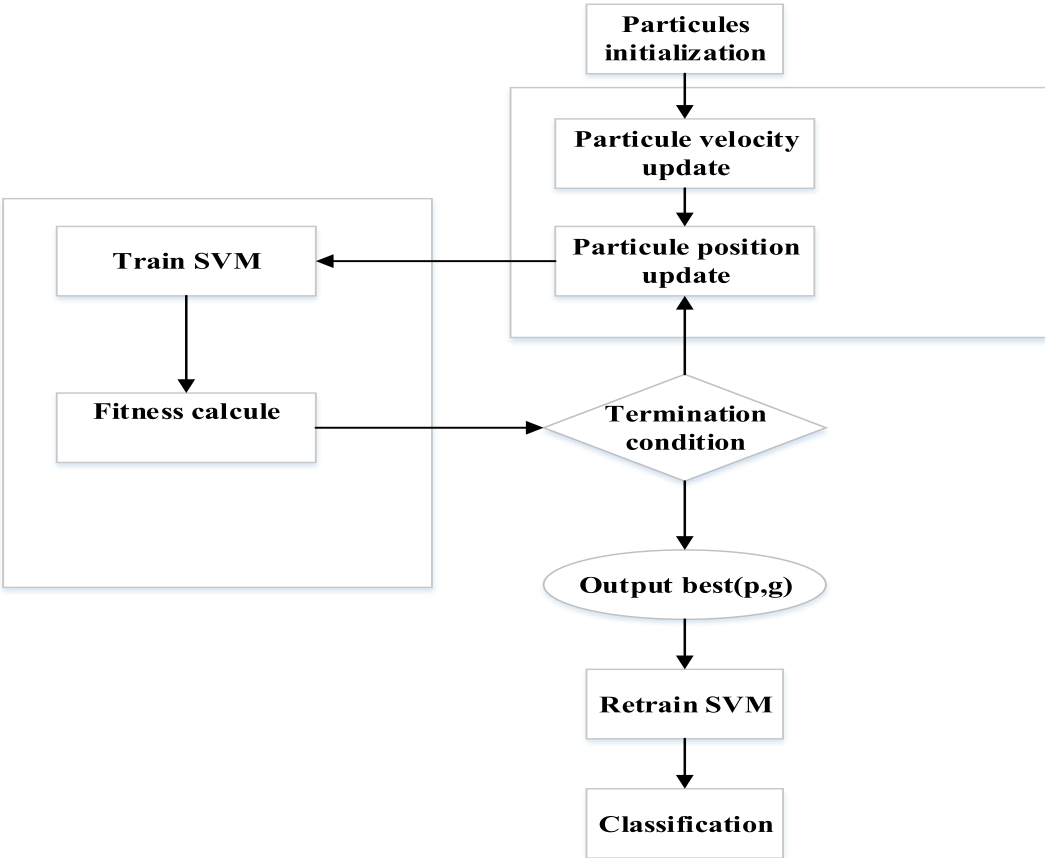

Fig. 5. Flowchart of PSO-SVM method

was included in more than one set. This prevented data leaks and made performance metrics appear better than they actually were. Stratified sampling was also employed to maintain the original class distribution in all subsets. Within the training set, we used 5-fold cross-validation to build the model and adjust the hyper parameters, particularly the regularization parameter C for the SVM and the gamma parameter for the RBF kernel. This step is a critical part of the PSO process. We used the validation set to monitor the optimization process and establish criteria for stopping early and avoiding overfitting. The PSO-optimized C parameter controlling the SVM's built-in regularization, which meant that finding a balance between margin complexity and classification error was necessary.

IV. Results

This study introduces the findings of using PSO-optimized SVM for the classification of epileptic seizures and compares it with standard approaches. Furthermore, we investigated the consequences of these findings within the framework of EEG and ECG signal analysis. The experiments, involving preprocessing, feature extraction, classifier optimization, and classification, were performed using MATLAB. We have successfully implemented the binary classification algorithm to differentiate between seizure and non-seizure events. We categorized a particular 960-second section of ECG and EEG data, dividing it into 96 segments. The learning and training phase comprised 72 recordings, constituting three-quarters of the total recordings. We allocated the remaining 24 recordings, which make up one-fourth of the total, for the testing and evaluation phase. We trained the algorithm on a total of 72 signals. Of these, 13 signals showed signs of a seizure, while the remaining 59 signals showed signs of a normal seizure. We obtained four vectors after performing the discrete wavelet decomposition mentioned above: D1, D2, D3, and D4. They corresponded to the first, second, third, and fourth levels, respectively. The training procedure is now complete. The last stage involves assessing the algorithm's capacity to distinguish between the two groups by including supplementary segments. We used a collection of 24 instances to achieve this goal, of which 11 are similar to epileptic cases and the remaining 13 fall into the non-seizure category.

The resulting performance was analyzed in terms of accuracy, specificity, and recall (sensitivity), which are

Manuscript received 12 June 2025; Revised 25 August 2025; Accepted 10 September 2025; Available online 30 September 2025
Digital Object Identifier (**DOI**): https://doi.org/10.35882/jeeemi.v7i3.1159
Copyright © 2025 by the authors. This work is an open-access article and licensed under a Creative Commons Attribution-ShareAlike 4.0 International License (CC BY-SA 4.0).

Journal of Electronics, Electromedical Engineering, and Medical Informatics
Homepage: jeeemi.org; Vol. 7, No. 4, October 2025, pp: 1144-1157 e-ISSN: 2656-8632

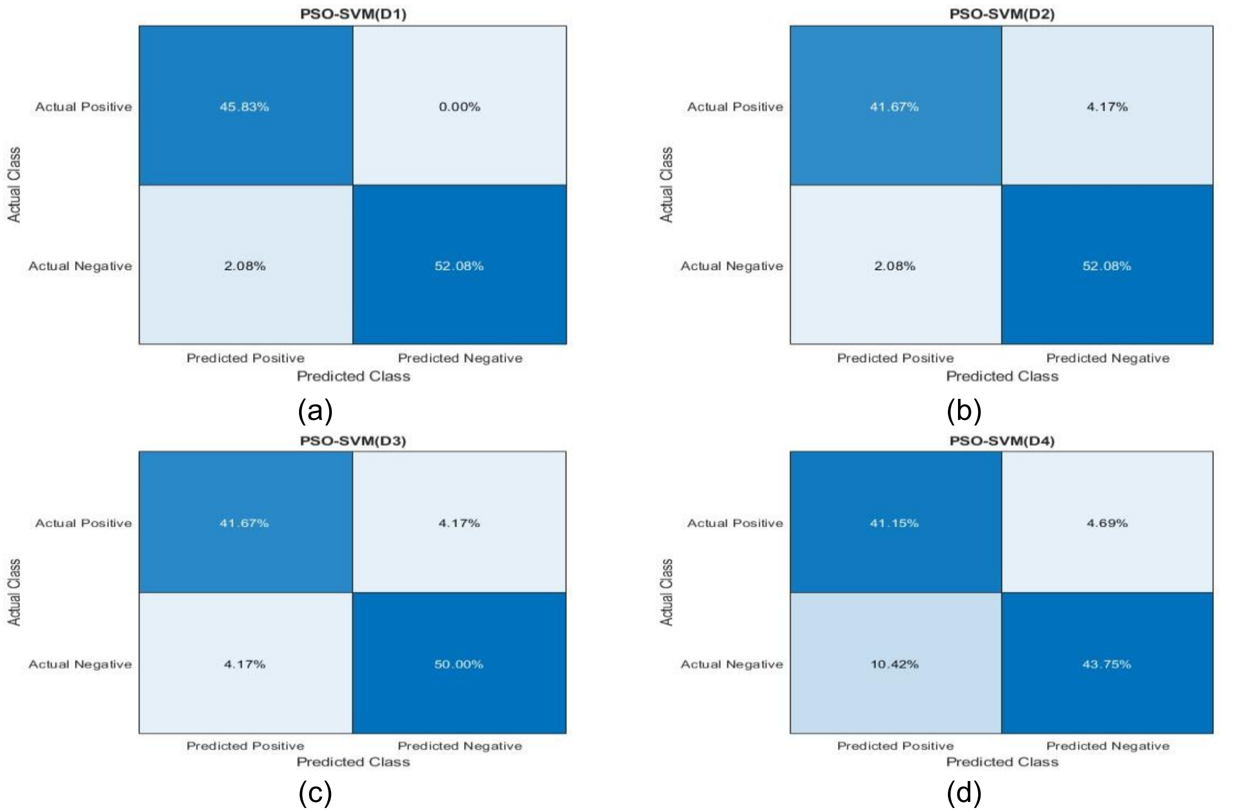

Fig. 6. Confusion matrices (a) PSO-SVM(D1)**, (b)** PSO-SVM(D2)**, (c)** PSO-SVM(D3)**, (d)** PSO-SVM(D4)

defined by Eq. (20) [39], Eq. (21) [40], and Eq. (22) [41], respectively, as follows:

$$Acc = \frac{TN + TP}{TN + TP + FP + FN}\ (\%) \tag{20}$$

$$Spe = \frac{TN}{TN+FP}\ (\%) \tag{21}$$

$$Rec = \frac{TP}{TP+FN}\ (\%) \tag{22}$$

TP is data with a positive number in the True Actual class that is correctly classified in the Positive Prediction class. TN is data with a negative number in the True Actual class that is correctly classified in the Negative Prediction class. FP is data with a negative False Class Sum that is incorrectly classified in the Positive Prediction class. FN is data with a positive False Class Sum that is incorrectly classified in the Negative Prediction class [42].

Table 2 illustrates the performance of the algorithm before optimizing the parameters of the SVM classifier. We found the most accurate result for D1, the characteristics vector of the first detail factor of the DWT. This indicates that the crisis primarily impacted the detail 1 coefficients. Table 3 illustrates the algorithm's performance subsequent to the implementation of the PSO optimization approach. D1, representing the feature vector of the initial coefficient from the DWT, consistently attains the maximum accuracy.

Table 2. Effectiveness of the algorithm without optimization

Results	Recall (%)	Specificity (%)	Accuracy (%)	AUC
SVM(D1)	95.65	92.31	94.44	0.92
SVM(D2)	91.3	88.89	90.41	-
SVM(D3)	91.49	80	87.5	-
SVM(D4)	89.36	80	86.11	-

Table 3. Effectiveness of the algorithm using optimization

Results	Recall (%)	Spec. (%)	Acc. (%)	AUC
PSO-SVM (D1)	100	96.15	97.92	0.96
PSO-SVM (D2)	91.3	96.15	93.75	-
PSO-SVM (D3)	91.3	92.31	91.67	-
PSO-SVM (D4)	89.36	80.77	84.9	-

Manuscript received 12 June 2025; Revised 25 August 2025; Accepted 10 September 2025; Available online 30 September 2025
Digital Object Identifier (**DOI**): https://doi.org/10.35882/jeeemi.v7i3.1159
Copyright © 2025 by the authors. This work is an open-access article and licensed under a Creative Commons Attribution-ShareAlike 4.0 International License (CC BY-SA 4.0).

Journal of Electronics, Electromedical Engineering, and Medical Informatics
Homepage: jeeemi.org; Vol. 7, No. 4, October 2025, pp: 1144-1157 e-ISSN: 2656-8632

V. Discussion

A synthetic statistical validation was performed based on the reported recall, specificity, and accuracy to see how strong the reported performance metrics were. Using binomial sampling, we performed more than 1,000 simulated runs to determine 95% confidence intervals for each metric. PSO-SVM(D1), for example, had a mean accuracy of 97.92%, a 95% confidence interval of (97.4%, 99.7%), a 100% recall, and a 96.15% specificity. Similar analyses on other SVM and PSO-SVM models confirmed the statistical significance of the observed enhancements, highlighting the stability and reliability of the proposed methodology despite limited data availability.

The PSO-optimized SVM clearly outperforms the non-optimized variant on all criteria. The system demonstrates accuracy, sensitivity, and specificity above 90%, indicating its capacity to accurately distinguish between epileptic and non-epileptic cases. To assess the classifier's capacity to differentiate between classes, the confusion matrices presented in Fig. 6 and ROC curves for the SVM and PSO SVM datasets were generated. Fig. 7 indicate that the proximity of the graph to the left and top of the coordinate axes correlates with enhanced classification efficacy.

A better classifier performance corresponds to an increased area under the curve. The AUC value of the PSO-SVM method surpasses that of the SVM alone. Fig. 8 presents a PSO convergence curve of the optimized SVM parameters using EEG-ECG features. The PSO runs for 100 iterations, and the plot of the curve shows that between 0 and 20 iterations, the fitness value drops rapidly. After 20 iterations, the fitness began to stabilize.

Table 4 compares the performance of the proposed particle swarm optimization (PSO)-support vector machine (SVM) combined with discrete wavelet transform (DWT) against several recent studies in epileptic seizure detection. Alalayah et al. (2023) [4] reported an accuracy of 97.36% using a random forest classifier combined with PCA and Kmeans. They achieved a recall of 92.98% and a specificity of 98.32. Pattnaik et al. (2022) [12] employed a tunable-Q wavelet transform with machine learning classifiers and attained an accuracy of 93% and a recall of 91.5%. However, they did not explicitly report the specificity values. Mporas et al. (2015) [23] demonstrated the benefits of multimodal EEG–ECG fusion with an SVM classifier, achieving a high recall of 99.9% and an overall accuracy of 96.11%, though the specificity was slightly lower at 92.31%. In comparison, the current study achieved a superior balance of metrics with perfect recall (100%), high specificity (96.15%), and high overall accuracy (97.92%). These results highlight the effectiveness of combining PSO-based parameter optimization with SVM and DWT feature extraction. This approach achieved state-of-the-art accuracy and demonstrates robustness in seizure detection across sensitivity and specificity. Unlike approaches that rely on additional data modalities (EEG–ECG fusion) or complex dimensionality reduction, the proposed method achieved comparable or superior performance with a more streamlined, computationally efficient

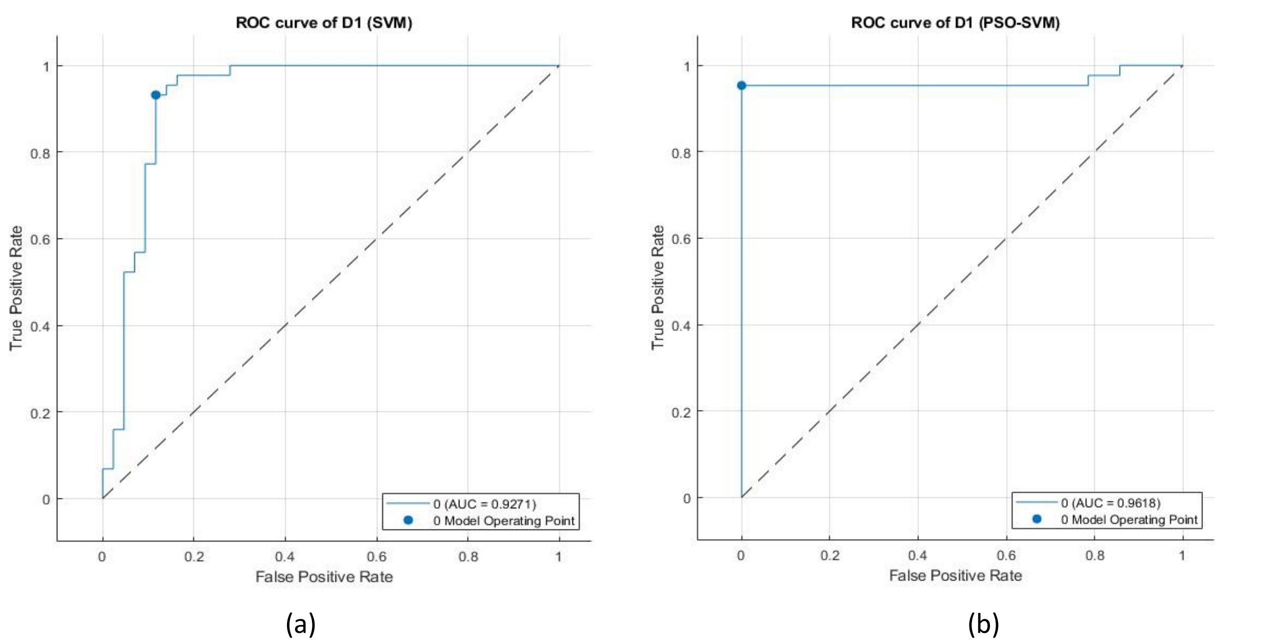

Fig. 7. ROC curve results (a) ROC curve without optimization (b) ROC curve with optimization

Manuscript received 12 June 2025; Revised 25 August 2025; Accepted 10 September 2025; Available online 30 September 2025
Digital Object Identifier (**DOI**): https://doi.org/10.35882/jeeemi.v7i3.1159
Copyright © 2025 by the authors. This work is an open-access article and licensed under a Creative Commons Attribution-ShareAlike 4.0 International License (CC BY-SA 4.0).

Table 4. Comparison with related work

Study	Method	Recall (%)	Specificity (%)	Accuracy (%)
Alalayah et al., 2023 [4]	RF+PCA+Kmeans	92.9	98.3	97.36
Pattnaik et al., 2022 [12]	Tunable-Q Wavelet Transform + ML	91.5	-	93
Mporas et al. (2015) [23]	EEG+ECG fusion+SVM	99.9	92.31	96.11
Current study	PSO-SVM+DWT	100	96.15	97.92

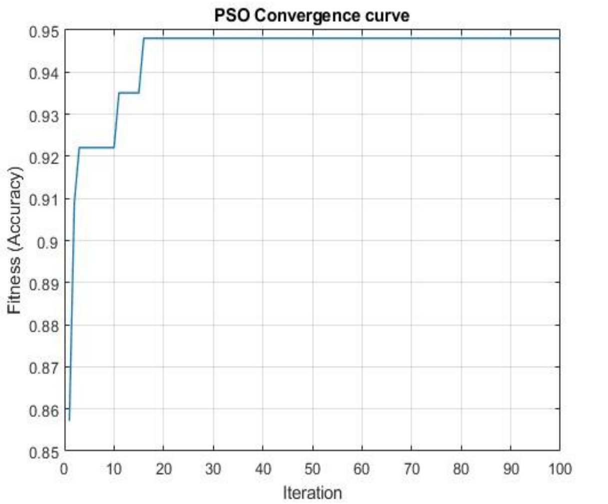

Fig. 8. PSO convergence curve

design. This highlights its potential for scalable, real-time clinical applications. Despite the positive outcomes, it is crucial to recognize the constraints of this research. First, the limited sample size of the dataset may limit the model's ability to be used in other situations and increase the likelihood that it will fit too closely to the data, despite the strategies used to avoid this (cross-validation and regularization). Second, validation was performed on only one dataset. Future work should include external validation on independent, multicenter datasets to test robustness and reduce any biases specific to the original dataset. Lastly, the model's performance may be suboptimal in other recording settings with different hardware or patient groups. Therefore, more testing is needed before the model can be used in clinical settings.

VI. Conclusion

The aim of the study was the development of a robust PSO-SVM framework for the classification of ECG and EEG signals by automating the critical selection of SVM hyper parameters. The study's success in achieving this aim is evident. The findings confirm that moving beyond default settings is essential for maximizing classifier performance. Our PSO algorithm was optimized to minimize the number of support vectors for greater efficiency and identified optimal parameters (C and γ), leading to a significant performance boost. The PSO-SVM model achieved a classification accuracy of 97.92% on the test dataset, with a recall of 100% and a Specificity of 96.15%. This substantially outperforms the baseline SVM model, which used default parameters. This high recall rate is critical for medical applications because it ensures a low false negative rate. These results validate the framework's potential to capture nuanced information from DWT-based features and offer healthcare practitioners a reliable tool for tasks such as assessing epileptic foci. Future work will focus on large-scale, real-time clinical validation, integration with wearable monitoring systems, and exploration of advanced deep learning hybrids. These efforts aim to extend the framework's capabilities beyond classification to include proactive seizure prediction, thereby enhancing its direct impact on patient care.

Acknowledgment

The authors would like to express their gratitude for the editor's and reviewers' insightful feedback and valuable suggestions. These contributions have greatly helped to improve the clarity and rigor of the manuscript. We would also like to thank our colleagues at the LSIB Laboratory for their continuous support.

Funding

This research received no specific grant from any funding agency in the public, commercial, or not-for-profit sectors.

Data Availability

The dataset used during this study is available in the CHB-MIT Scalp EEG Database, at https://doi.org/10.13026/C2K01R.

Author Contribution

ZOUGAGH designed and conceptualized the study. ZOUGAGH and NAHID contributed to the writing and revision of the manuscript. ZOUGAGH and BOUYGHF assisted with data analysis and interpretation. All authors reviewed and approved the final version of the manuscript.

Declarations

Ethical Approval

Not applicable.

Manuscript received 12 June 2025; Revised 25 August 2025; Accepted 10 September 2025; Available online 30 September 2025
Digital Object Identifier (**DOI**): https://doi.org/10.35882/jeeemi.v7i3.1159
Copyright © 2025 by the authors. This work is an open-access article and licensed under a Creative Commons Attribution-ShareAlike 4.0 International License (CC BY-SA 4.0).

Consent for Publication Participants.
Consent for publication was given by all participants

Competing Interests
The authors declare no competing interests.

References

[1] N. Margolese, A. Badeghiesh, H. Baghlaf, S. Jacobson, and M. H. Dahan, "Maternal epilepsy and pregnancy, delivery and neonatal outcomes: A population-based retrospective cohort study," Epilepsy & Behavior, 163, p. 110221. https://doi.org/10.1016/j.yebeh.2024.110221.

[2] World Health Organization, "Global status report on alcohol and health 2018," World Health Organization, Geneva, 2018.

[3] C. De Stefano, F. Fontanella, C. Marrocco, and A. Scotto Di Freca, "A GA-based feature selection approach with an application to handwritten character recognition," Pattern Recognition Letters, vol. 35, no. 1, pp. 130–141, Jan. 2014, doi: 10.1016/j.patrec.2013.01.026.

[4] Alalayah, K.M.; Senan, E.M.; Atlam, H.F.; Ahmed, I.A.; Shatnawi, H.S.A. Effective Early Detection of Epileptic Seizures through EEG Signals Using Classification Algorithms Based on t-Distributed Stochastic Neighbor Embedding and K-Means. Diagnostics 2023, 13, 1957. https://doi.org/10.3390/diagnostics13111957.

[5] Das, S.; Mumu, S.A.; Akhand, M.A.H.; Salam, A.; Kamal, M.A.S. Epileptic Seizure Detection from Decomposed EEG Signal through 1D and 2D Feature Representation and Convolutional Neural Network. Information 2024, 15, 256. https://doi.org/10.3390/info15050256.

[6] K. M. Hassan, Md. R. Islam, T. Tanaka, and Md. K. I. Molla, "Epileptic Seizure Detection from EEG Signals Using Multiband Features with Feedforward Neural Network," in 2019 International Conference on Cyberworlds (CW), Oct. 2019, pp. 231–238. doi: 10.1109/CW.2019.00046.

[7] A. Sharma, S. Rani, and M. Driss, "Hybrid evolutionary machine learning model for advanced intrusion detection architecture for cyber threat identification," PLOS ONE, vol. 19, no. 9, p. e0308206, Sep. 2024, doi: 10.1371/journal.pone.0308206.

[8] T. Shawly et al., "LHAENA: Lightweight Hybrid Attention Ensemble Network Architecture for Epileptic Seizure Detection," Journal of Disability Research, vol. 4, p. 20250581, Jul. 2025, doi: 10.57197/JDR-2025-0581.

[9] S. Qiu, W. Wang, and H. Jiao, "LightSeizureNet: A Lightweight Deep Learning Model for Real-Time Epileptic Seizure Detection," IEEE Journal of Biomedical and Health Informatics, vol. 27, no. 4, pp. 1845–1856, Apr. 2023, doi: 10.1109/JBHI.2022.3223970.

[10] A. A. Ein Shoka, M. M. Dessouky, A. El-Sayed, and E. E.-D. Hemdan, "EEG seizure detection: concepts, techniques, challenges, and future trends," Multimed Tools Appl, vol. 82, no. 27, pp. 42021–42051, Nov. 2023, doi: 10.1007/s11042-023-15052-2.

[11] F. Ok, R. Rajesh, F. Ok, and R. Rajesh, "Empirical Mode Decomposition of EEG Signals for the Effectual Classification of Seizures," in Advances in Neural Signal Processing, IntechOpen, 2020. doi: 10.5772/intechopen.89017.

[12] S. Pattnaik, N. Rout, and S. Sabut, "Machine learning approach for epileptic seizure detection using the tunable-Q wavelet transform based time–frequency features," Int. j. inf. tecnol., vol. 14, no. 7, pp. 3495–3505, Dec. 2022, doi: 10.1007/s41870-022-00877-1.

[13] K. M. Hassan, Md. R. Islam, T. T. Nguyen, and Md. K. I. Molla, "Epileptic seizure detection in EEG using mutual information-based best individual feature selection," Expert Systems with Applications, vol. 193, p. 116414, May 2022, doi: 10.1016/j.eswa.2021.116414.

[14] H. S. Nogay and H. Adeli, "Detection of Epileptic Seizure Using Pretrained Deep Convolutional Neural Network and Transfer Learning," European Neurology, vol. 83, no. 6, pp. 602–614, Jan. 2021, doi: 10.1159/000512985.

[15] S. Benbadis, S. Beniczky, E. Bertram, S. MacIver, and S. L. Moshé, "The role of EEG in patients with suspected epilepsy," Epileptic Disorders, vol. 22, no. 2, pp. 143–155, 2020, doi: 10.1684/epd.2020.1151.

[16] Aayesha, M. Bilal Qureshi, M. Afzaal, M. Shuaib Qureshi, and J. Gwak, "Fuzzy-Based Automatic Epileptic Seizure Detection Framework," Computers, Materials & Continua, vol. 70, no. 3, pp. 5601–5630, 2022, doi: 10.32604/cmc.2022.020348.

[17] M. Sameer and B. Gupta, "CNN based framework for detection of epileptic seizures," Multimed Tools Appl, vol. 81, no. 12, pp. 17057–17070, May 2022, doi: 10.1007/s11042-022-12702-9.

[18] J. He, J. Cui, G. Zhang, M. Xue, D. Chu, and Y. Zhao, "Spatial–temporal seizure detection with graph attention network and bi-directional LSTM architecture," Biomedical Signal Processing and Control, vol. 78, p. 103908, Sep. 2022, doi:

Manuscript received 12 June 2025; Revised 25 August 2025; Accepted 10 September 2025; Available online 30 September 2025
Digital Object Identifier (**DOI**): https://doi.org/10.35882/jeeemi.v7i3.1159
Copyright © 2025 by the authors. This work is an open-access article and licensed under a Creative Commons Attribution-ShareAlike 4.0 International License (CC BY-SA 4.0).

10.1016/j.bspc.2022.103908.

[19] R. Sharma and H. K. Meena, "Emerging Trends in EEG Signal Processing: A Systematic Review," SN COMPUT. SCI., vol. 5, no. 4, pp. 1–14, Apr. 2024, doi: 10.1007/s42979-024-02773-w.

[20] N. S. Amer and S. B. Belhaouari, "EEG Signal Processing for Medical Diagnosis, Healthcare, and Monitoring: A Comprehensive Review," IEEE Access, vol. 11, pp. 143116–143142, 2023, doi: 10.1109/ACCESS.2023.3341419.

[21] S. Bouazizi and H. Ltifi, "Enhancing accuracy and interpretability in EEG-based medical decision making using an explainable ensemble learning framework application for stroke prediction," Decision Support Systems, vol. 178, p. 114126, Mar. 2024, doi: 10.1016/j.dss.2023.114126.

[22] F. Mason et al., "Heart Rate Variability as a Tool for Seizure Prediction: A Scoping Review," Journal of Clinical Medicine, vol. 13, no. 3, p. 747, Jan. 2024, doi: 10.3390/jcm13030747.

[23] I. Mporas, V. Tsirka, E. I. Zacharaki, M. Koutroumanidis, M. Richardson, and V. Megalooikonomou, "Seizure detection using EEG and ECG signals for computer-based monitoring, analysis and management of epileptic patients," Expert Systems with Applications, vol. 42, no. 6, pp. 3227–3233, Apr. 2015, doi: 10.1016/j.eswa.2014.12.009.

[24] Ali Hossam Shoeb, "Application of machine learning to epileptic seizure onset detection and treatment," Massachusetts Institute of Technology, 2009. [Online]. Available: http://dspace.mit.edu/handle/1721.1/7582

[25] A. L. Goldberger et al., "PhysioBank, PhysioToolkit, and PhysioNet: components of a new research resource for complex physiologic signals," Circulation, vol. 101, no. 23, pp. E215-220, Jun. 2000, doi: 10.1161/01.cir.101.23.e215.

[26] J. Guttag, CHB-MIT Scalp EEG Database (version 1.0.0). PhysioNet, 2010. doi: 10.13026/C2K01R.

[27] E. Ali, M. Angelova, and C. Karmakar, "Epileptic seizure detection using CHB-MIT dataset: The overlooked perspectives," R Soc Open Sci, vol. 11, no. 5, p. 230601, doi: 10.1098/rsos.230601.

[28] E. Alickovic, J. Kevric, and A. Subasi, "Performance evaluation of empirical mode decomposition, discrete wavelet transform, and wavelet packed decomposition for automated epileptic seizure detection and prediction," Biomedical Signal Processing and Control, vol. 39, pp. 94–102, Jan. 2018, doi: 10.1016/j.bspc.2017.07.022.

[29] S. C. Ks, A. Mishra, V. Shirhatti, and S. Ray, "Comparison of Matching Pursuit Algorithm with Other Signal Processing Techniques for Computation of the Time-Frequency Power Spectrum of Brain Signals," J. Neurosci., vol. 36, no. 12, pp. 3399–3408, Mar. 2016, doi: 10.1523/JNEUROSCI.3633-15.2016.

[30] L. Zougagh, H. Bouyghf, M. Nahid, and I. Sabiri, "A New Approach for Epileptic Seizure Detection from EEG and ECG Signals Using Wavelet Decomposition," in International Conference on Advanced Intelligent Systems for Sustainable Development (AI2SD'2023), Springer, Cham, 2024, pp. 370–378. doi: 10.1007/978-3-031-52388-5_33.

[31] P. S. Addison, The Illustrated Wavelet Transform Handbook: Introductory Theory and Applications in Science, Engineering, Medicine and Finance, Second Edition, 2nd ed. Boca Raton: CRC Press, 2017. doi: 10.1201/9781315372556.

[32] I. Mporas, V. Tsirka, E. I. Zacharaki, M. Koutroumanidis, M. Richardson, and V. Megalooikonomou, "Seizure detection using EEG and ECG signals for computer-based monitoring, analysis and management of epileptic patients," Expert Systems with Applications, vol. 42, no. 6, pp. 3227–3233, Apr. 2015, doi: 10.1016/j.eswa.2014.12.009.

[33] L. Zougagh, H. Bouyghf, M. Nahid, and I. Sabiri, "Epilepsy detection using wavelet transform, genetic algorithm, and decision tree classifier," IAES International Journal of Artificial Intelligence (IJ-AI), vol. 13, no. 3, Art. no. 3, Sep. 2024, doi: 10.11591/ijai.v13.i3.pp3447-3455.

[34] D. N. Joanes and C. A. Gill, "Comparing measures of sample skewness and kurtosis," *Journal of the Royal Statistical Society: Series D (The Statistician)*, vol. 47, no. 1, pp. 183–189, 1998, doi: 10.1111/1467-9884.00122.

[35] X. Yan and M. Jia, "A novel optimized SVM classification algorithm with multi-domain feature and its application to fault diagnosis of rolling bearing," Neurocomputing, vol. 313, pp. 47–64, Nov. 2018, doi: 10.1016/j.neucom.2018.05.002.

[36] Y. Zhong, H. Wei, L. Chen, and T. Wu, "Automated EEG Pathology Detection Based on Significant Feature Extraction and Selection," Mathematics, vol. 11, no. 7, p. 1619, Jan. 2023, doi: 10.3390/math11071619.

[37] J. Kennedy and R. C. Eberhart, "A discrete binary version of the particle swarm algorithm," in Computational Cybernetics and Simulation

Manuscript received 12 June 2025; Revised 25 August 2025; Accepted 10 September 2025; Available online 30 September 2025
Digital Object Identifier (**DOI**): https://doi.org/10.35882/jeeemi.v7i3.1159
Copyright © 2025 by the authors. This work is an open-access article and licensed under a Creative Commons Attribution-ShareAlike 4.0 International License (CC BY-SA 4.0).

Journal of Electronics, Electromedical Engineering, and Medical Informatics
Homepage: jeeemi.org; Vol. 7, No. 4, October 2025, pp: 1144-1157 e-ISSN: 2656-8632

1997 IEEE International Conference on Systems, Man, and Cybernetics, Oct. 1997, pp. 4104–4108 vol.5. doi: 10.1109/ICSMC.1997.637339.

[38] Z.-S. Chen, B. Zhu, Y.-L. He, and L.-A. Yu, "A PSO based virtual sample generation method for small sample sets: Applications to regression datasets," Engineering Applications of Artificial Intelligence, vol. 59, pp. 236–243, Mar. 2017, doi: 10.1016/j.engappai.2016.12.024.

[39] L. Zougagh, H. Bouyghf, M. Nahid, and B. Ouacha, "Feature extraction and classification of epileptic seizures from combined EEG and ECG signals," J. Phys.: Conf. Ser., vol. 2550, no. 1, p. 012028, Aug. 2023, doi: 10.1088/1742-6596/2550/1/012028.

[40] Y. Zhong, H. Wei, L. Chen, and T. Wu, "Automated EEG Pathology Detection Based on Significant Feature Extraction and Selection," Mathematics, vol. 11, no. 7, p. 1619, Jan. 2023, doi: 10.3390/math11071619.

[41] E. Juárez-Guerra, V. Alarcon-Aquino, and P. Gómez-Gil, "Epilepsy Seizure Detection in EEG Signals Using Wavelet Transforms and Neural Networks," in New Trends in Networking, Computing, E-learning, Systems Sciences, and Engineering, Springer, Cham, 2015, pp. 261–269. doi: 10.1007/978-3-319-06764-3_33.

[42] J. Xu, Y. Zhang, and D. Miao, "Three-way confusion matrix for classification: A measure driven view," Information Sciences, vol. 507, pp. 772–794, Jan. 2020, doi: 10.1016/j.ins.2019.06.064.

Author Biography

Zougagh Lahcen received his license degree in Biomedical Instrumentation and Maintenance from the Institute of Health Sciences (ISSS) at the University Hassan I Settat-Morocco in 2018 and then a Master's degree in biomedical engineering from FMPM Marrakech in 2020. He is currently a Ph.D. student at Hassan II University in Mohammedia-Casablanca, Morocco, in the Laboratory of Engineering Sciences and Biosciences (LSIB). Under the direction of Pr. M. Nahid, Professor in the Electrical Engineering Department at the same university, his research and interests are centered on the development, design, and optimization of electronic systems for biomedical engineering and health sciences. He can be contacted at email: lahcen.zougagh-etu@etu.univh2c.ma.

Bouyghf Hamid was born in Errachidia, Morocco, in 1982. He got his B.S. and M.S. degrees in Electrical Engineering and Telecom from the University of Science and Technology in Fez, Morocco, in 2007, and his Ph.D. in Electrical Engineering and Telecom from Hassan II University of Casablanca, Morocco, in 2019. From 2015 until 2019, he worked as a Research Assistant at the Princeton Plasma Physics Laboratory. Since 2019, he has worked as an Assistant Professor at the Electrical Engineering Department of Hassan II University's FST Mohammedia in Casablanca, Morocco. In the topic of IC optimization, he has written numerous articles. His research interests include biomedical electronics, analog IC design, electromagnetic fields, low power design, and BLE applications. He can be contacted at email: hamid.bouyghf@gmail.com

Nahid Mohammed studied electronics and received the B.S diploma in Electronics at ENSET Institute, Mohammedia, Morocco in 1994, received the Aggregation diploma of electronics and electrical engineering, from ENSET institute of Rabat, Morocco in 2000. He received the DESA diploma in computer engineering, telecoms and multimedia in 2004. He conducted doctoral research at images, videos coding and quality assessment under psychovisual quality criteria since 2004 at Mohamed V university of Rabat, Morocco, where he received his Ph.D. in 2010. Dr. Nahid, which is research professor in the Faculty of Science and Technology of Mohammedia since 2011, conducts research on visual perception and its application to coding, understanding, and display of visual information and to human vision, image quality, and digital imaging. Research and projects are also focused on artificial intelligence, embedded systems, biomedical systems, smart grids, digital and analog IC design. He can be contacted at email: mohammed.nahid@gmail.com.

Manuscript received 12 June 2025; Revised 25 August 2025; Accepted 10 September 2025; Available online 30 September 2025
Digital Object Identifier (**DOI**): https://doi.org/10.35882/jeeemi.v7i3.1159
Copyright © 2025 by the authors. This work is an open-access article and licensed under a Creative Commons Attribution-ShareAlike 4.0 International License (CC BY-SA 4.0).